


Poly *N,N*-dimethylaniline-formaldehyde supported on silica-coated magnetic nanoparticles: a novel and retrievable catalyst for green synthesis of 2-amino-3-cyanopyridines

Sajad Asadbegi¹ · Mohammad Ali Bodaghifard^{1,2}  · Akbar Mobinikhaledi¹

Received: 14 July 2017 / Accepted: 11 November 2017 / Published online: 23 November 2017
© Springer Science+Business Media B.V., part of Springer Nature 2017

Abstract Preparation and application of novel and reusable magnetic nanoparticles with poly *N,N*-dimethylaniline-formaldehyde support as a heterogeneous basic catalyst have been described. The reported catalyst was characterized by Fourier transform infrared spectroscopy, scanning electron microscopy, X-ray diffraction patterns, transmission electron microscopy, energy dispersive X-ray spectroscopy, thermogravimetric analysis and vibrating sample magnetometry. The catalytic performance of this organic-inorganic hybrid nanomaterial has been studied for the green synthesis of 2-amino-3-cyanopyridine derivatives through one-pot four-component reactions. An eco-friendly method, short reaction time, high yield and easy work-up procedure are the advantages of this new methodology over earlier ones.

Keywords 2-Amino-3-cyanopyridines · Magnetic nanoparticles · Multi-component reactions · Green synthesis

Introduction

Nitrogen-containing heterocycles play important roles in biology. They have an important place among natural and synthetic products because of their special properties as key elements of various drugs [1]. The pyridine nucleus has appeared

Electronic supplementary material The online version of this article (<https://doi.org/10.1007/s11164-017-3200-4>) contains supplementary material, which is available to authorized users.

✉ Mohammad Ali Bodaghifard
mbodaghi2007@yahoo.com; m-bodaghifard@araku.ac.ir

¹ Department of Chemistry, Faculty of Science, Arak University, Arak 38156-88349, Iran

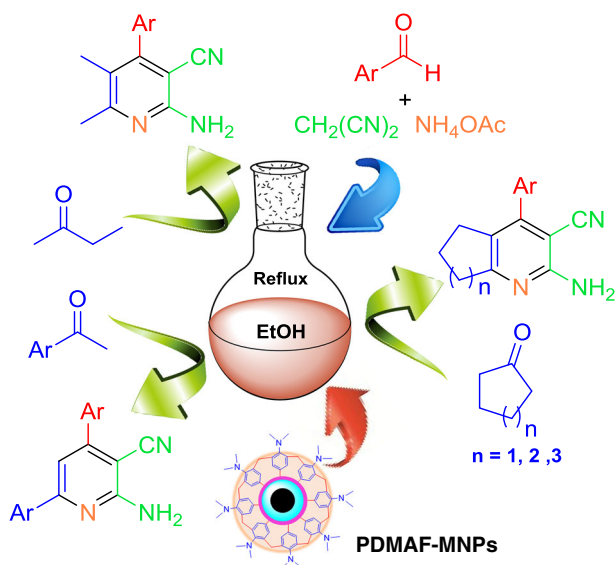
² Institute of Nanosciences and Nanotechnology, Arak University, Arak 38156-88349, Iran

as a privileged scaffold in view of its spread in numerous pharmaceuticals, natural products and functional materials [2, 3]. Pyridines are also involved in supramolecular structures [4], materials and surfaces [5], coordination chemistry [6] and organocatalysis [7]. Polysubstituted pyridines are significant because such scaffolds constitute structures of many organic functional materials and natural products [8, 9].

Among them, 2-amino-3-cyanopyridine derivatives have attracted important attention due to their biological activities such as antibacterial [10], antiviral [11], antimicrobial [12], antifungal [13], anti-inflammatory [14] and antitumor [15] properties. They are known as adenosine receptor antagonists, potent inhibitors of HIV-1 integrase [16], IKK-b inhibitors [17] and antiexcitotoxic agents [18]. Therefore, development of synthetic methodologies for the preparation of 2-amino-3-cyanopyridine derivatives from readily available substrates under mild reaction conditions continues to attract much interest in organic chemistry [19].

The synthetic methods for preparation of numerous types of 2-amino-3-cyanopyridine derivatives include utilization of corresponding 2-chloro derivatives as substrates [20], reaction of chalcones with ammonium acetate [21], condensation of arylidene malononitrile, ketones and ammonium acetate [22] and one-pot four-component reactions [23–28]. However, some of these reported procedures have limitations such as the use of toxic solvents [18], expensive metal catalysts [2], harsh reaction conditions [29] and complicated reaction and work-up procedures [30].

Heterogeneous catalysis is of superb importance in several areas of the energy-consuming and chemical industries [31–33]. Nanocatalysts are more efficient than normal heterogeneous catalysts due to their extremely small size and great surface area-to-volume ratio [34]. In the past decade, considerable attention has been paid to the Fe₃O₄ magnetic nanoparticles (MNPs) in several different fields due to their unrivaled properties such as biocompatibility, low toxicity, high surface area, superparamagnetic behavior and adaptability for large-scale production [35, 36]. Above all, the Fe₃O₄ MNPs are simply produced and can be easily separated by an external magnet from the reaction mixture and reused [37]. Due to the strong dipole–dipole attraction, pure Fe₃O₄ MNPs tend to form large aggregates. Large cluster formations have limited functional groups and lose their special properties [38]. Coating a silica layer on MNPs improves the performance and stability of these nanomaterials [39, 40]. Furthermore, functionalization of silica-coated nanoparticles can be conjugated with a range of various chemical entities and promote their use in numerous chemical processes [41–45]. In our continued interest on preparation and application of functionalized MNPs [46–48], we wish to report a highly efficient process for the synthesis of 2-amino-3-cyanopyridine derivatives via one-pot multi-component reactions using novel and designed poly *N,N*-dimethylaniline-formaldehyde supported on silica-coated Fe₃O₄ MNPs (PDMAF-MNPs) as a catalyst under green conditions (Scheme 1).



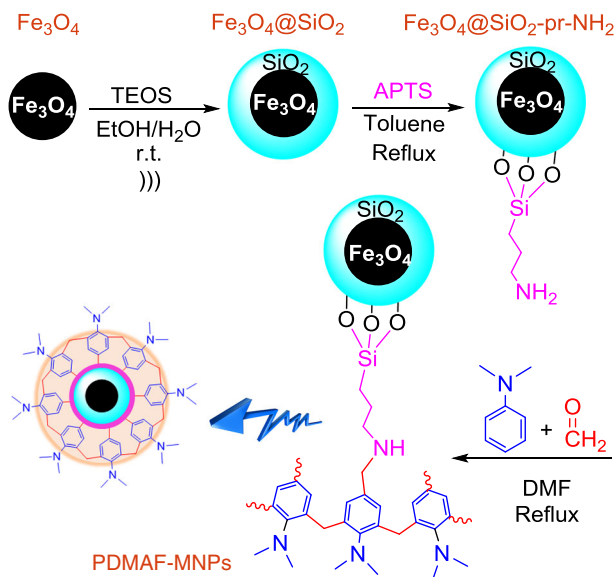
Scheme 1 The synthesis of 2-amino-3-cyanopyridine derivatives using novel poly *N,N*-dimethylaniline-formaldehyde supported on silica-coated Fe_3O_4 magnetic nanoparticles (PDMAF-MNPs) as an efficient catalyst

Results and discussion

Characterization of novel PDMAF-MNPs catalyst

PDMAF supported on silica-coated MNPs was prepared via the procedure demonstrated in Scheme 2. Fourier transform infrared (FT-IR) spectroscopy, field emission scanning electron microscopy (FE-SEM), energy dispersive X-ray spectroscopy (EDS), transmission electron microscopy (TEM), vibrating sample magnetometry (VSM), X-ray diffraction (XRD) and thermogravimetric analysis (TGA) were used to identify and characterize the green, mild, safe and novel magnetic catalyst.

The FT-IR of bare Fe_3O_4 MNPs, $\text{Fe}_3\text{O}_4@\text{SiO}_2$ core-shell MNPs (silica-coated MNPs), $\text{Fe}_3\text{O}_4@\text{SiO}_2\text{-pr-NH}_2$ (3-aminopropyl-functionalized silica-coated MNPs) and PDMAF-MNPs are shown in Fig. 1. In curve 1a, the spectrum of Fe_3O_4 nanoparticles relevant to the bending vibration of Fe–O shows an absorption around 578 cm^{-1} . Absorption bond appearance at 1096 cm^{-1} (asymmetric stretching), 955 cm^{-1} (symmetric stretching), 815 cm^{-1} (in-plane bending) and 457 cm^{-1} (rocking mode) for the Si–O–Si group confirms the formation of an SiO_2 shell (Fig. 1b). The twisting vibration mode of H–O–H adsorbed in the silica shell displays a weak band at 1615 cm^{-1} , and the stretching vibration mode of Si–OH appeared as a broad band in the range $3200\text{--}3500\text{ cm}^{-1}$. Alkyl group moieties are confirmed by the weak bands at 2935 and 2960 cm^{-1} related to C–H symmetric and asymmetric stretching modes (Fig. 1c, d). Furthermore, bands appearing at $1450\text{--}1650\text{ cm}^{-1}$ (C=C in aromatic rings) indicate formation of PDMAF (Fig. 1d).



Scheme 2 Preparation of novel poly *N,N*-dimethylaniline-formaldehyde supported on silica-coated Fe_3O_4 magnetic nanoparticles (PDMAF-MNPs)

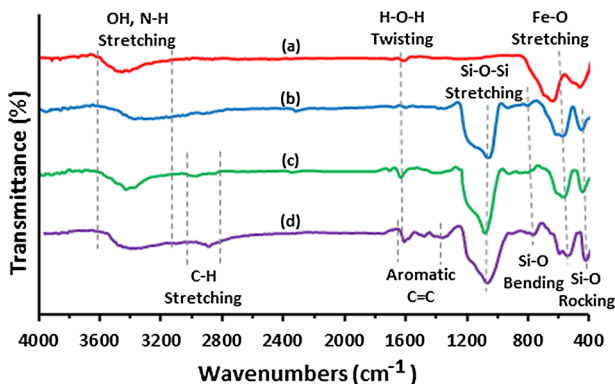


Fig. 1 The FT-IR spectrum of **a** Fe_3O_4 , **b** $\text{Fe}_3\text{O}_4@\text{SiO}_2$, **c** $\text{Fe}_3\text{O}_4@\text{SiO}_2\text{-pr-NH}_2$ and **d** PDMAF-MNPs

Therefore, the achieved results show that the materials are added in each section and the MNP catalyst is formed successfully.

FE-SEM was used to determine the size and morphology of the prepared PDMAF-MNPs catalyst (Fig. 2a). PDMAF-MNPs, as can be seen in Fig. 2a, have a mean diameter of about 20–30 nm and have a nearly spherical shape, indicating the nanocatalyst has a large surface area. TEM analysis shows a grey silica shell about 5–10 nm thick on a dark Fe_3O_4 core which indicates silica is successfully anchored to the MNPs, and the average size of the synthesized nanoparticles is 15–30 nm (Fig. 2b).

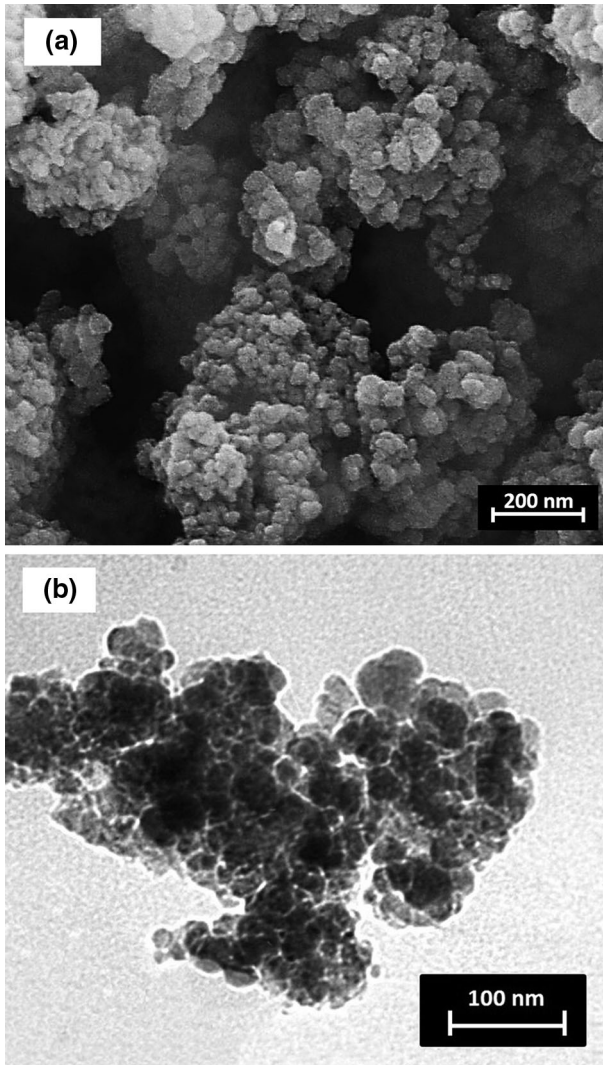


Fig. 2 a FE-SEM image and b TEM image of PDMAF-MNPs

EDS analysis indicates the presence of N and C in the PDMAF-MNPs (Fig. 3). Additionally, the presence of Si, O and Fe signals confirms that the iron oxide particles are loaded into the silica. The higher intensity of the Si and O peaks compared with the Fe peaks indicates that the Fe_3O_4 nanoparticles were trapped by SiO_2 .

The crystalline structures of Fe_3O_4 and PDMAF-MNPs were studied by XRD (Fig. 4). The relative intensities and position of all peaks agree well with the standard XRD pattern of Fe_3O_4 (JCPDS card no. 85-1436), indicating retention of the crystalline cubic spinel structure during the silica coating procedure and

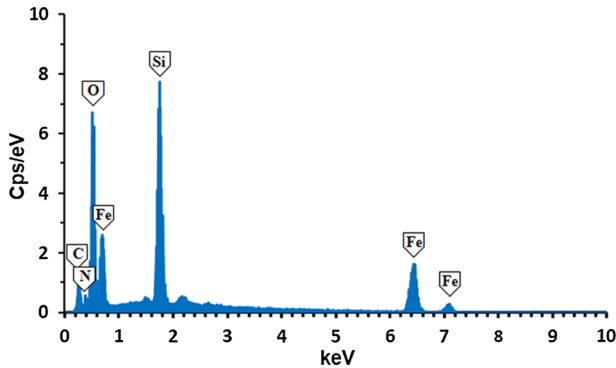


Fig. 3 EDS spectrum of PDMAF-MNPs nanocatalyst

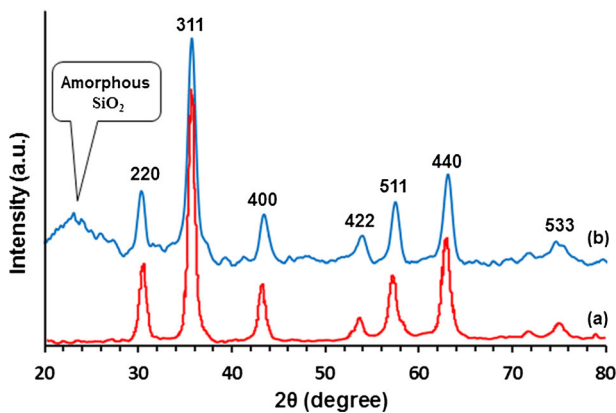


Fig. 4 XRD patterns of **a** Fe₃O₄ MNPs and **b** PDMAF-MNPs

functionalization of MNPs. The characteristic peaks at $2\theta = 30.2^\circ$, 35.7° , 43.2° , 53.6° , 57.1° , 62.8° and 74.4° for pure Fe₃O₄ nanoparticles, which were marked respectively by their indices (220), (311), (400), (422), (511), (440) and (533) were also observed for Fe₃O₄ and PDMAF-MNPs [49]. This shown that modification on the surface of Fe₃O₄ nanoparticles did not lead to their phase change. The mean size of the crystallites was calculated by applying Scherrer's equation: $D = 0.9\lambda/\beta \cos\theta$, where λ is the wavelength of the X-rays, β is the broadening of the diffraction line measured at half of its maximum intensity in radians, θ is the Bragg diffraction angle and D is the average diameter in Å. The peak at $2\theta = 35.7^\circ$ is selected to calculate the crystallite size, according to the result calculated by Scherrer's equation, it is found that the diameter of PDMAF-MNPs obtained is about 21 nm which is in the range determined using FE-SEM and TEM analysis (Fig. 2).

The TGA curve of PDMAF-MNPs showed an initial weight loss up to 235 °C, which was attributed to the removal of physically adsorbed solvent and surface hydroxyl groups (Fig. 5). The major weight loss beyond about 235 °C to nearly 575 °C is attributed to the decomposition of the organic moiety in the

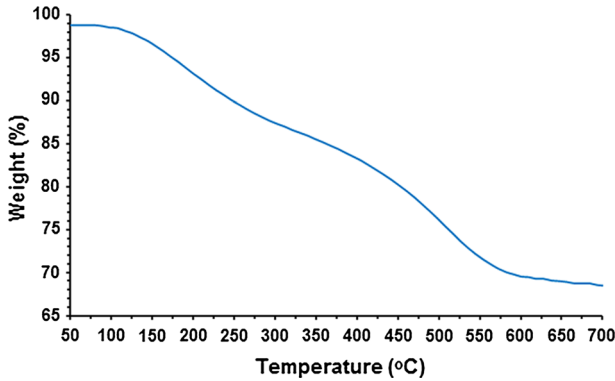


Fig. 5 TGA curves of PDMAF-MNPs

nanocomposite. Therefore, the catalyst is reasonably stable up to 235 °C and it is safe to carry out the reaction under heterogeneous conditions. And so, this weight loss step gives the organic supported ratios of the magnetic catalyst and the PDMAF supported on the $\text{Fe}_3\text{O}_4@\text{SiO}_2$ MNPs was approximately 21 wt%.

The magnetic properties of Fe_3O_4 MNPs and PDMAF-MNPs were characterized by VSM. Figure 6 shows the typical room temperature magnetization curves of bare Fe_3O_4 MNPs (Fig. 6a), and PDMAF-MNPs (Fig. 6b). The hysteresis curve allows determination of the coercivity (H_c), remanent magnetization (M_r) and saturation magnetization (M_s). The magnetization of samples could be completely saturated at high fields of up to ± 8000.0 Oe and the M_s of samples changes from 53.5 to 31.1 emu g^{-1} due to the formation of a silica shell and organic layer around the Fe_3O_4 core. The hysteresis loops show the superparamagnetic behaviour of the Fe_3O_4 and PDMAF-MNPs in which M_r and H_c are close to zero ($M_r = 0.85$ and 1.15 emu g^{-1} and $H_c = 6.50$ and 11.85 Oe, respectively) [50].

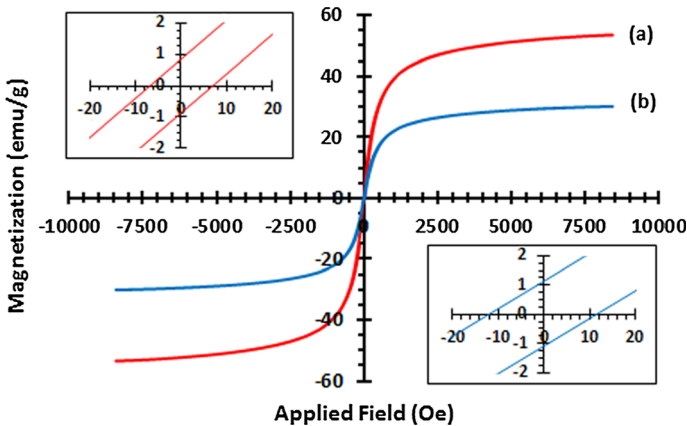


Fig. 6 Magnetic hysteresis loops of **a** Fe_3O_4 MNPs and **b** PDMAF-MNPs

Synthesis of 2-amino-3-cyanopyridine derivatives catalysed by PDMAF-MNPs

After characterization of the prepared PDMAF-MNPs, the catalytic activity of this nanomaterial was examined in the synthesis of 2-amino-3-cyanopyridine derivatives. To find the suitable reaction conditions, a one-pot four-component reaction of benzaldehyde **1a** (1 mmol), cyclohexanone **2a** (1 mmol), malononitrile **3** (1 mmol) and ammonium acetate **4** (1.5 mmol) was selected and examined as a model under a variety of conditions.

We used different solvents like acetonitrile, EtOH, THF and H₂O under reflux conditions. Results showed that ethanol serves as the best solvent with respect to having a green nature, polarity and clean workup procedure for this synthesis (Table 1, entry 2). For the synthesis completion, various amounts of PDMAF-MNPs displayed that 40 mg of the nanocatalyst is sufficient (Table 1, entry 5). By lowering the reaction temperature, the yield of the product was decreased to 68% (Table 1, entry 8). To define the role of PDMAF-MNPs as a catalyst for the preparation of 2-amino-3-cyanopyridine derivatives, the model reaction was carried out with Fe₃O₄, Fe₃O₄@SiO₂, *N,N*-dimethylaniline and without the catalyst (Table 1, entries 9–12). With respect to yield of product and reaction time, the best results are attained using PDMAF-MNPs as the catalyst.

Table 1 Optimization of reaction conditions for synthesis of 2-amino-3-cyanopyridine derivatives

Entry	Catalyst (mg)	Solvent	Temp. (°C)	Time (h)	Yield (%) ^a
1	PDMAF-MNPs (20)	CH ₃ CN	Reflux	3	75
2	PDMAF-MNPs (20)	EtOH	Reflux	3	86
3	PDMAF-MNPs (20)	THF	Reflux	3	78
4	PDMAF-MNPs (20)	H ₂ O	Reflux	3	71
5	PDMAF-MNPs (40)	EtOH	Reflux	2.5	92
6	PDMAF-MNPs (60)	EtOH	Reflux	2.5	88
7	PDMAF-MNPs (40)	EtOH	50	4	87
8	PDMAF-MNPs (40)	EtOH	r.t.	7	68
9	–	EtOH	Reflux	6	51
10	<i>N,N</i> -dimethylaniline	EtOH	Reflux	2	82
11	Fe ₃ O ₄	EtOH	Reflux	2.5	81
12	Fe ₃ O ₄ @SiO ₂	EtOH	Reflux	2.5	75

Reaction conditions: benzaldehyde (1 mmol), malononitrile (1 mmol), cyclohexanone (1 mmol), ammonium acetate (1.5 mmol)

^aIsolated yield; r.t. room temperature

Table 2 The synthesis of 2-amino-3-cyanopyridines using PDMAF-MNPs as a catalyst

Entry	Aldehyde	Ketone	Product	Time (h)	Yield (%) ^a	M.p. (°C) [Lit. Refs.]
1	Benzaldehyde	Cyclohexanone	5a	2.5	92	237–239 [234–235] [22]
2	4-Dimethylaminobenzaldehyde	Cyclohexanone	5b	3	86	245–247
3	3-Nitrobenzaldehyde	Cyclohexanone	5c	2	93	231–233 [230–232] [51]
4	4-Chlorobenzaldehyde	Cyclohexanone	5d	2	92	254–256 [258–259] [52]
5	4-Methoxybenzaldehyde	Cyclohexanone	5e	3	89	238–240 [232–234] [25]
6	Benzaldehyde	Cyclopentanone	5f	2.5	91	225–227 [220–221] [24]
7	4-Chlorobenzaldehyde	Cyclopentanone	5g	2	88	244–246
8	2,4-Dichlorobenzaldehyde	Cyclopentanone	5h	3	85	230–232
9	4-Dimethylaminobenzaldehyde	Cyclopentanone	5i	3	87	234–236
10	4-Methoxybenzaldehyde	Cyclopentanone	5j	3	90	220–222 [217–218] [22]
11	Benzaldehyde	Cycloheptanone	5k	2.5	88	221–223 [227–228] [53]
12	3-Nitrobenzaldehyde	Cycloheptanone	5l	2	90	213–215
13	2,4-Dichlorobenzaldehyde	Cycloheptanone	5m	3	78	228–230
14	4-Chlorobenzaldehyde	Cycloheptanone	5n	2	85	234–236
15	4-Methoxybenzaldehyde	Cycloheptanone	5o	3	83	223–225 [225–227] [25]
16	Benzaldehyde	Acetophenone	5p	1.5	89	181–183 [176–177] [54]
17	4-Chlorobenzaldehyde	Acetophenone	5q	2	85	234–236 [233–235] [55]
18	4-Methoxybenzaldehyde	Acetophenone	5r	2	82	179–181 [177–180] [56]
19	4-Nitrobenzaldehyde	Acetophenone	5s	1	86	222–224 [223–225] [57]
20	4-Methylbenzaldehyde	Acetophenone	5t	2	87	164–166 [160–161] [54]
21	Benzaldehyde	2-Butanone	5u	3	85	240–241 [240–241] [24]
22	2-Chlorobenzaldehyde	2-Butanone	5v	2.5	87	252–254 [251–252] [53]
23	4-Methoxybenzaldehyde	2-Butanone	5w	3.5	77	276–277 [275–277] [2]
24	4-Bromobenzaldehyde	2-Butanone	5x	2.5	79	265–266 [265–266] [24]

Table 2 continued

Entry	Aldehyde	Ketone	Product	Time (h)	Yield (%) ^a	M.p. (°C) [Lit. Refs.]
25	4-Methylbenzaldehyde	2-Butanone	5y	3.5	74	256–258 [259–260] [22]

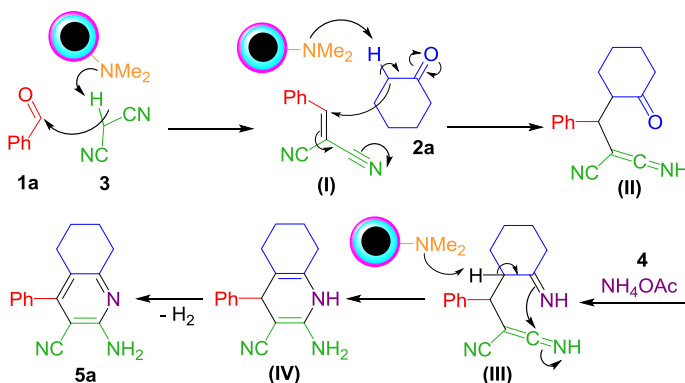
The bracketed values are reported melting points in literature

Reaction conditions: aldehyde (1 mmol), malononitrile (1 mmol), ketone (1 mmol), ammonium acetate (1.5 mmol)

^aIsolated yield; *M.p.* melting point

With the optimized reaction conditions in hand, we then assessed the substrate scope of this reaction. As shown in Table 2, various aldehydes reacted with malononitrile, ammonium acetate and ketone derivatives to give the corresponding 2-amino-3-cyanopyridines with good to excellent yields under optimized conditions. Arylaldehydes with electron-donating or electron-withdrawing groups could lead to the favored products **5a–y**. Aliphatic aldehydes were also used, but did not afford the desired products. As detailed in Table 2, electron-donating groups decrease the rate and hence increase the time of reaction, and electron-withdrawing groups increase the rate and decrease the reaction's time.

A possible mechanism for the synthesis of 2-amino-3-cyanopyridines catalysed with PDMAF-MNPs is shown in Scheme 3. The formation of 2-amino-4-phenyl-5,6,7,8-tetrahydroquinoline-3-carbonitrile (**5a**) can be rationalized by the initial formation of benzyldenemalononitrile (**I**) as an intermediate via the standard Knoevenagel condensation of benzaldehyde and malononitrile in the presence of PDMAF-MNPs as a catalyst. Michael addition of cyclohexanone (**2a**) to the activated double bond of the (**I**) provides adduct (**II**). Next, a nucleophilic attack of ammonium acetate (**4**) on the carbonyl group of (**III**) affords the intermediate (**IV**). Intramolecular cyclization of these intermediates following oxidation produced the target product (**5a**).



Scheme 3 Possible mechanism for the synthesis of compound **5a** using PDMAF-MNPs

Table 3 Comparison of PDMAF-MNPs with other catalysts described in the literature for the synthesis of 2-amino-4-phenyl-5,6,7,8-tetrahydroquinoline-3-carbonitrile

Entry	Catalyst	Condition	Time	Yield ^a (%)	Refs.
1	Fe ₃ O ₄ /cellulose nanoparticles	EtOH (r.t.)	3	90	[25]
2	Au/MgO	EtOH (70)	2.5	90	[58]
3	–	Benzene (reflux)	4	66	[22]
4	[Yb(PFO) ₃]	EtOH (reflux)	4	92	[2]
5	Fe ₃ O ₄ nanoparticles	Neat (80)	2.15	86	[26]
6	Graphene oxide	Water (80)	5	86	[27]
7	Cu/C nanocatalyst	Acetonitrile (80)	8	84	[54]
8	1-Butyl-3-methylimidazolium hydroxide	Ionic liquid (r.t.)	4	82	[51]
9	–	Trifluoroethanol (reflux)	6	80	[55]
10	PDMAF-MNPs	EtOH (reflux)	2.5	92	Present work

Reaction conditions: benzaldehyde (1 mmol), malononitrile (1 mmol), cyclohexanone (1 mmol), ammonium acetate (1.5 mmol)

^aIsolated yields; *r.t.* room temperature

To compare the applicability of our catalyst with other catalysts used for the synthesis of 2-amino-3-cyanopyridine derivatives, the results of these catalysts in the condensation reaction of benzaldehyde, malononitrile, cyclohexanone and ammonium acetate under optimized conditions have been tabulated in Table 3. As can be seen, the catalytic system reported in this paper has benefits in terms of simple conditions, short reaction times and excellent yields.

Catalyst recovery and reusability

Recyclability of this magnetic nanocatalyst was studied in the relation between benzaldehyde (1 mmol), malononitrile (1 mmol), cyclohexanone (1 mmol) and ammonium acetate (1.5 mmol). After accomplishment of the reaction, the nanocatalyst was recovered easily using an external magnet, washed successively with EtOH, double-distilled water and then dried. The catalyst could be used at least six times without significant loss of activity (Fig. 7). The XRD and FT-IR studies of the catalyst after six runs confirmed its stability. The recovered catalyst had no distinct change in structure, as apparent from a comparison of its XRD and FT-IR spectra with that of fresh catalyst (Fig. 8).

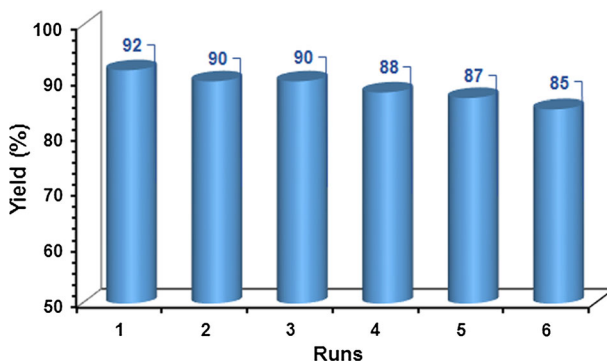


Fig. 7 Recyclability of PDMAF-MNPs in the synthesis of 2-amino-3-cyanopyridines

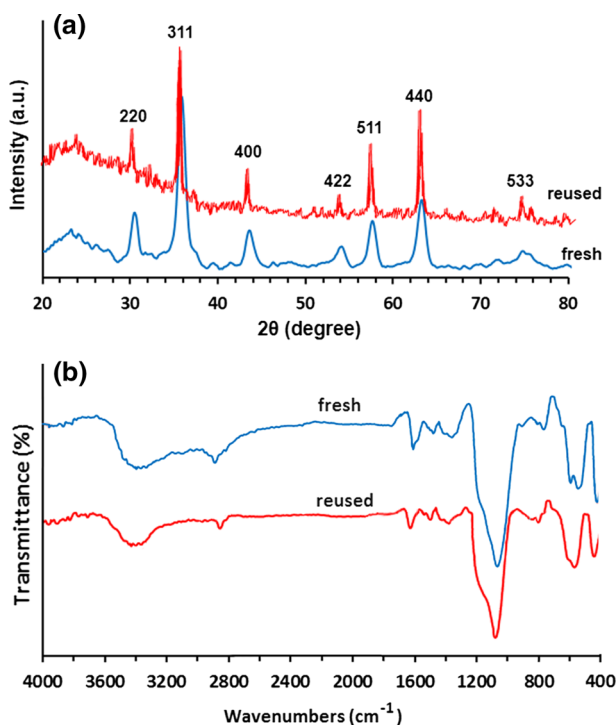


Fig. 8 a XRD and b FT-IR spectra of fresh catalyst and that reused six times

Conclusions

In this study, a green and efficient process has been developed for synthesis of 2-amino-3-cyanopyridine derivatives using PDMAF-MNPs as a novel, efficient and recyclable magnetic catalyst. The nanocatalyst was characterized using FT-IR spectroscopy, FE-SEM, XRD, TEM, VSM, EDS and TGA. The noticeable features

of this method are simple workup procedure, short reaction time and high yield. Various ketones and aromatic aldehydes led to the corresponding 2-amino-3-cyanopyridines in good to excellent yields. In all reactions, the catalyst could be easily isolated using an external magnetic field and recovered for six times without significant loss of activity.

Experimental

General procedure for preparation of PDMAF-MNPs

In the beginning, Fe_3O_4 MNPs were synthesized by using the chemical co-precipitation of Fe^{3+} and Fe^{2+} ions as defined in the literature [59]. Typically, $\text{FeCl}_3 \cdot 6\text{H}_2\text{O}$ (10 mmol) and $\text{FeCl}_2 \cdot 4\text{H}_2\text{O}$ (5 mmol) were dissolved in 100 ml of deionized water. The mixture was heated in an N_2 atmosphere and at a temperature of 80 °C for 1 h, and then 10 ml of concentrated ammonia (25%) was quickly injected into the reaction mixture in one portion. The solution was stirred under N_2 for another 1 h and then cooled to room temperature. The black precipitate was collected by magnetic decantation, washed with distilled water until neutrality, washed and dried at 60 °C under vacuum. Surfaces of the MNPs with a layer of silica were covered by using the Stöber method [60]. Fe_3O_4 MNPs (1.0 g) were homogeneously dispersed with 25 wt% concentrated aqueous ammonia solution (1.5 ml) in a mixture of ethanol (40 ml) followed by the addition of 1.4 ml of tetraethylorthosilicate (TEOS). After stirring for 12 h under an N_2 atmosphere at room temperature, the $\text{Fe}_3\text{O}_4@ \text{SiO}_2$ was isolated from the solution, washed and dried at 25 °C under vacuum. In the following, aminopropyl-modified silica-coated Fe_3O_4 MNPs were synthesized according to the described procedure [61]. In 50 ml of dry toluene, 1.0 g of $\text{Fe}_3\text{O}_4@ \text{SiO}_2$ MNPs was dispersed using an ultrasonic bath to yield a uniform suspension, and using a syringe, 2.0 g of 3-aminopropyl-trimethoxysilane (APTS) was then added. The mixture was stirred for 48 h at 60 °C under an N_2 atmosphere. The aminopropyl-functionalized solid $\text{Fe}_3\text{O}_4@ \text{SiO}_2$ -pr- NH_2 MNPs were washed with toluene, separated and then dried under vacuum. Finally, *N,N*-dimethylaniline (5 mmol) and formaldehyde (10 mmol) dissolved in 50 ml of DMF was added to 1 g of $\text{Fe}_3\text{O}_4@ \text{SiO}_2$ -pr- NH_2 and the mixture was refluxed for 24 h. Obtained hybrid nanoparticles named as PDMAF-MNPs were collected, washed and dried.

General procedure for the synthesis 2-amino-3-cyanopyridines catalysed by PDMAF-MNPs

Aldehyde (1.0 mmol), malononitrile (1.0 mmol), ketone (1.0 mmol) and ammonium acetate (1.5 mmol) were dissolved in EtOH (10 ml), and PDMAF-MNPs (40 mg) were added to a round-bottomed flask equipped with a magnetic stir bar and a condenser. The mixture was stirred and refluxed for the appropriate time detailed in Table 2. Progress of the reaction was monitored by thin-layer chromatography (TLC). After completion of the reaction, the catalyst was recovered

from the reaction mixture by using an external magnet. The corresponding solid product **5** was obtained with the addition of water to the mixture, and recrystallized from EtOH affording the pure 2-amino-3-cyanopyridines. The recovered PDMAF-MNPs were washed with EtOH, distilled water, dried under reduced pressure and reused.

Acknowledgements We gratefully acknowledge the financial support of this work by the research council of Arak University.

References

1. V. Polshettiwar, R.S. Varma, *Pure Appl. Chem.* **80**, 777 (2008)
2. J. Tang, L. Wang, Y. Yao, L. Zhang, W. Wang, *Tetrahedron Lett.* **52**, 509 (2011)
3. N.M. Evdokimov, A.S. Kireev, A.A. Yakovenko, M.Y. Antipin, I.V. Magedov, A. Kornienko, *J. Org. Chem.* **72**, 3443 (2007)
4. T. Šmejkal, B. Breit, *Angew. Chem.* **120**, 317 (2008)
5. R. Makiura, S. Motoyama, Y. Umemura, H. Yamanaka, O. Sakata, H. Kitagawa, *Nat. Mater.* **9**, 565 (2010)
6. D. Bora, B. Deb, A.L. Fuller, A.M. Slawin, J.D. Woollins, D.K. Dutta, *Inorg. Chim. Acta* **363**, 1539 (2010)
7. N. De Rycke, F. Couty, O.R. David, *Chem. Eur. J.* **17**, 12852 (2011)
8. L. Jayasinghe, C.P. Jayasooriya, N. Hara, Y. Fujimoto, *Tetrahedron Lett.* **44**, 8769 (2003)
9. C. Temple Jr., G.A. Rener, W.R. Waud, P.E. Noker, *J. Med. Chem.* **35**, 3686 (1992)
10. S.G. Konda, V. Khedkar, B. Dawane, *J. Chem. Pharm. Res.* **2**, 187 (2010)
11. A.E.G. Hammam, N.A.A. El-hafeza, W.H. Midurab, M. Mikolajczyk, *Z. Naturforsch. Pt. B* **55**, 417 (2000)
12. D.C. Mungra, M.P. Patel, R.G. Patel, *Arkivoc* **14**, 64 (2009)
13. A.R. Gholap, K.S. Toti, F. Shirazi, R. Kumari, M.K. Bhat, M.V. Deshpande, K.V. Srinivasan, *Bioorg. Med. Chem. Lett.* **15**, 6705 (2007)
14. T. Murata, M. Shimada, S. Sakakibara, T. Yoshino, T. Masuda, T. Shintani, H. Sato, Y. Koriyama, K. Fukushima, N. Nunami, *Bioorg. Med. Chem. Lett.* **14**, 4019 (2004)
15. F. Zhang, Y. Zhao, L. Sun, L. Ding, Y. Gu, P. Gong, *Eur. J. Med. Chem.* **46**, 3149 (2011)
16. J. Deng, T. Sanchez, L.Q. Al-Mawsawi, R. Dayam, R.A. Yunes, A. Garofalo, M.B. Bolger, N. Neamati, *Bioorg. Med. Chem. Lett.* **15**, 4985 (2007)
17. T. Murata, M. Shimada, S. Sakakibara, T. Yoshino, H. Kadono, T. Masuda, M. Shimazaki, T. Shintani, K. Fuchikami, K. Sakai, *Bioorg. Med. Chem. Lett.* **13**, 913 (2003)
18. A. Girgis, A. Kalmouch, H. Hosni, *Amino Acids* **26**, 139 (2004)
19. M.A. Bodaghifard, M. Solimannejad, S. Asadbegi, S. Dolatabadifarahani, *Res. Chem. Intermed.* **42**, 1165 (2015)
20. R. Galeeva, E. Rudometova, M.Y. Gavrilov, V. Kolla, M. Kon'shin, F.Y. Nazmetdinov, *Pharm. Chem. J.* **31**, 89 (1997)
21. A. Sakurai, H. Midorikawa, *Bull. Chem. Soc. Jpn* **41**, 430 (1968)
22. S. Kambe, K. Saito, A. Sakurai, H. Midorikawa, *Synthesis* **1980**, 366 (1980)
23. A. Mobinikhaledi, S. Asadbegi, M.A. Bodaghifard, *Synth. Commun.* **19**, 1605 (2016)
24. S. Kankala, R. Pagadala, S. Maddila, C.S. Vasam, S.B. Jonnalagadda, *RSC Adv.* **5**, 105446 (2015)
25. B. Maleki, S. Sheikh, *Org. Prep. Proced. Int.* **47**, 368 (2015)
26. M.M. Heravi, S.Y.S. Beheshtiha, M. Dehghani, N. Hosseintash, *J. Iran. Chem. Soc.* **12**, 2075 (2015)
27. D. Khalili, *Tetrahedron Lett.* **57**, 1721 (2016)
28. M. Álvarez-Pérez, J. Marco-Contelles, *Arkivoc* **2**, 283 (2011)
29. F. Shi, S. Tu, F. Fang, T. Li, *Arkivoc* **1**, 137 (2005)
30. T.R. Reddy, G.R. Reddy, L.S. Reddy, S. Jammula, Y. Lingappa, R. Kapavarapu, C.L.T. Meda, K.V. Parsa, M. Pal, *Eur. J. Med. Chem.* **48**, 265 (2012)
31. R. Swathi, K. Sebastian, *Resonance* **13**, 548 (2008)
32. S. Roy, K.K. Senapati, P. Phukan, *Res. Chem. Intermed.* **41**, 5753 (2015)

33. W. Zhou, J. Yi, J. Lin, S. Fang, X. Peng, *Res. Chem. Intermed.* **43**, 3651 (2017)
34. V. Polshettiwar, T. Asefa, G. Hutchings, *Nanocatalysis: Synthesis and Applications* (Wiley, New York, 2013)
35. J. Dobson, *Drug Dev. Res.* **67**, 55 (2006)
36. Q.A. Pankhurst, J. Connolly, S.K. Jones, J. Dobson, *J. Phys. D Appl. Phys.* **36**, R167 (2003)
37. M.M. Khodaei, A. Alizadeh, M. Haghypour, *Res. Chem. Intermed.* (2017). <https://doi.org/10.1007/s11164-017-3008-2>
38. S. Sun, H. Zeng, *J. Am. Chem. Soc.* **124**, 8204 (2002)
39. M.A. Zolfigol, R. Ayazi-Nasrabadi, *RSC Adv.* **6**, 69595 (2016)
40. B. Zakerinasab, M. Nasserri, H. Hassani, M. Samieadel, *Res. Chem. Intermed.* **42**, 3169 (2016)
41. Y. Lu, Y. Yin, B.T. Mayers, Y. Xia, *Nano Lett.* **2**, 183 (2002)
42. W. Wu, Q. He, C. Jiang, *Nanoscale Res. Lett.* **3**, 397 (2008)
43. M. Butterworth, L. Illum, S. Davis, *Colloid Surf. A* **179**, 93 (2001)
44. S. Santra, R. Tapeç, N. Theodoropoulou, J. Dobson, A. Hebard, W. Tan, *Langmuir* **17**, 2900 (2001)
45. M. Pramanik, A. Bhaumik, *ACS Appl. Mater. Interfaces.* **6**, 933 (2014)
46. M.A. Bodaghifard, A. Mobinikhaledi, S. Asadbegi, *Appl. Organomet. Chem.* **31**, e3557 (2016)
47. M.A. Bodaghifard, S. Asadbegi, Z. Bahrami, *J. Iran. Chem. Soc.* **14**, 365 (2016)
48. M.A. Bodaghifard, Z. Faraki, A.R. Karimi, *Curr. Org. Chem.* **20**, 1648 (2016)
49. G. Feng, D. Hu, L. Yang, Y. Cui, X.-A. Cui, H. Li, *Sep. Purif. Technol.* **74**, 253 (2010)
50. K. Petcharoen, A. Sirivat, *Mater. Sci. Eng., B* **177**, 421 (2012)
51. Y. Wan, R. Yuan, F.-R. Zhang, L.-L. Pang, R. Ma, C.-H. Yue, W. Lin, W. Yin, R.-C. Bo, H. Wu, *Synth. Commun.* **41**, 2997 (2011)
52. O. El-Salam, D. Ella, N. Ismail, M. Abdullah, *Pharmazie* **64**, 147 (2009)
53. R. Pagadala, S. Maddila, S. Jonnalagadda, *J. Heterocycl. Chem.* **52**, 1226 (2015)
54. R. Khalifeh, M. Ghamari, *J. Braz. Chem. Soc.* **27**, 759 (2016)
55. S. Khaksar, M. Yaghoobi, *J. Fluor. Chem.* **142**, 41 (2012)
56. Q. Wu, Y. Zhang, S. Cui, *Org. Lett.* **16**, 1350 (2014)
57. M.A. Zolfigol, M. Kiafar, M. Yarie, A.A. Taherpour, M. Saeidi-Rad, *RSC Adv.* **6**, 50100 (2016)
58. R. Pagadala, S. Maddila, V. Moodley, W.E. van Zyl, S.B. Jonnalagadda, *Tetrahedron Lett.* **55**, 4006 (2014)
59. K. Can, M. Ozmen, M. Ersoz, *Colloid Surf. B* **71**, 154 (2009)
60. W. Stöber, A. Fink, E. Bohn, *J. Colloid Interface Sci.* **26**, 62 (1968)
61. T. Zeng, L. Yang, R. Hudson, G. Song, A.R. Moores, C.-J. Li, *Org. Lett.* **13**, 442 (2010)